Time-Resolved Resonance Raman Study of the Triplet State of the *p*-Hydroxyphenacyl Acetate Model Phototrigger Compound

Chensheng Ma, Wing Sum Chan, Wai Ming Kwok, Peng Zuo, and David Lee Phillips*

Department of Chemistry, The University of Hong Kong, Pokfulam Road, Hong Kong SAR, People's Republic of China

Received: November 26, 2003; In Final Form: March 5, 2004

Picosecond and nanosecond time-resolved resonance Raman spectroscopy have been used to study the dynamics and structure of the phototrigger compound *p*-hydroxyphenacyl acetate (HPA) in acetonitrile solution. An intermediate was observed that exhibited significant quenching by oxygen. This intermediate was identified and attributed to the $\pi\pi^*$ triplet state of HPA. Temporal evolution at early picosecond times indicates rapid intersystem crossing conversion and subsequent relaxation of the excess energy of the initially formed triplet state. B3LYP/6-311G** density functional theory (DFT) calculations were done to determine the structures and vibrational frequencies for both the HPA triplet and ground states. The experimental and theoretical results were compared and discussed in relation to the initial pathway for the *p*-hydroxyphenacyl deprotection reaction and the nature of the triplet state relative to other aromatic carbonyl compounds. The present results demonstrate the utility of applying ultrafast vibrational spectroscopy to study the mechanism of the photorelease process in phototrigger compounds.

Introduction

The *p*-hydroxyphenacyl group was recently found to be a new and efficient photoremovable group for various biological stimulants in aqueous solution.[1−9] This new class of phototrigger compounds has been proposed for use as the second generation of the α-keto "cage" phototrigger compounds due to its superior properties compared to the commonly used *o*-nitrobenzyl cage[1−3] and desyl cage[1−4] compounds. For example, the *p*-hydroxyphenacyl cage is an improvement over the *o*-nitrobenzyl cage in terms of having a rapid release rate of the desired functional group and is also free of complicated side reactions.[1−3] The *p*-hydoxyphenacyl cage is also an improvement over the desyl cage with regard to having a good aqueous buffer solubility and not containing a chiral center.[1−4] Studies by Givens and co-workers have demonstrated that these *p*-hydroxyphenacyl ester compounds can serve as efficient phototriggers for the rapid and localized liberation of inorganic phosphate,[3,4,8,9] peptides,[5,6] oligopeptides,[6] amino acids,[5−7] and nucleotides,[6,9] etc., from the corresponding *p*-hydroxyphenacyl caged esters after UV excitation. The photochemical deprotection occurs with high quantum efficiency (∼0.3) and a very high rate of $\sim 10^7-10^8$ s^{-1}; the reaction is accompanied by a concomitant rearrangement of the protecting group into *p*-hydroxyphenylacetic acid in aqueous media.[3−9]

The practical applications of *p*-hydroxyphenacyl cage have led to much current interest in better understanding the mechanism(s) responsible for the photodeprotection process and the rearrangement reaction. Different mechanisms have been proposed in the literature, and there remain conflicting interpretations and controversies about how these processes occur for different molecules and environmental conditions. On the basis of quenching measurements, Givens and co-workers suggested that the lowest triplet is the reactive excited state leading to the subsequent release of the protected groups and the rearrangement of the phenacyl nucleus.[2−9] However, this assertion was later questioned by Wan and co-workers, and a singlet mechanism was proposed.[10,11] Wan and co-workers suggested that the primary photochemical step is a formal intramolecular proton transfer of the phenolic proton to the ketone carbonyl from the singlet excited state, the so-called excited-state intramolecular proton transfer (ESIPT), and they argued that ESIPT competes effectively with the intersystem crossing (ISC) to the excited triplet state. Falvey and co-workers recently performed a laser flash photolysis study on the photorelease mechanism of a phenacyl ester compound lacking the *p*-hydroxy group.[12] They concluded that the reaction follows a triplet mechanism and pointed out that hydrogen abstraction from solvent by the triplet carbonyl oxygen leading to generation of a ketyl radical, rather than the C−O bonding homolysis cleavage,[3,13,14,15] is the initial step for the photocleavage reaction. More recent work by Givens and co-workers[8] tends to confirm the short-lived triplet is the precursor to the chemical pathway leading to the rearrangement and cleavage of the leaving group, whose detailed mechanism still remains open for investigation. It is thus clear that further work is needed to better elucidate the overall reaction pathway and to clearly identify the reactive intermediates as well as to better clarify the validity of the reaction mechanisms suggested so far.

Direct structural and kinetic information on the intermediates involved in the reaction are essential for a better understanding of the processes related to the phenacyl deprotection, and this requires time-resolved measurements. Most previous time-resolved studies employed techniques such as transient absorption with nanosecond time resolution.[8,10−12] Valuable information has been obtained from these studies. For example, several transient species have been recognized on the basis of their measured lifetimes and different solvent-dependent kinetic behavior.[8,11] However, there has been no structural evidence available, and explicit identification of the putative reactive

* Author to whom correspondence should be addressed. FAX: 852-2857-1586. E-mail: Phillips@hku.hk.

10.1021/jp0376020 CCC: $27.50
Published on Web 05/29/2004

intermediates is still lacking. Such information is key to establish the reaction mechanism and clarify the related ambiguity in the reaction mechanisms proposed thus far. In addition, limitations imposed by most experiments to date provide little information about an ultrafast photophysical or photochemical process occurring immediately after photoexcitation of the molecule. It is well-known that time-resolved resonance Raman (TR^3) spectroscopy is a very powerful diagnostic approach to identify and monitor the kinetics of a short-lived reactive intermediate produced in various photoexcited processes.[13−23] This method yields direct structural information and can distinguish among multiple and similar intermediates having overlapping absorption spectra. In this sense, the technique is particularly suitable for investigating the phenacyl photo-deprotection reaction since previous transient absorption work found that the intermediates involved show strongly overlapping absorption bands.[8,10,11] By detecting directly the structure and kinetics of the transient species using the TR^3 method, our long-term goal seeks to construct the overall mechanism for the phenacyl deprotection and rearrangement reaction. We report here our preliminary results on the triplet state of *p*-hydroxyphenacyl acetate (HPA) obtained by picosecond and nanosecond TR^3 measurements. Since ISC rates are generally rapid for aryl carbonyl compounds[24−27] and the singlet excited-state proton transfer could also occur on the picosecond or even femtosecond time scale,[28−36] access to the picosecond time regime is essential for detecting early time dynamics and these results are expected to be helpful in differentiating the triplet and ESIPT singlet proposed mechanisms mentioned above. To our knowledge, this is the first time-resolved vibrational spectroscopy reported for the phenacyl phototrigger compounds.

Besides the intriguing applications as a protecting group for biological stimulants, HPA is also an interesting substituted aromatic carbonyl compound with regard to the nature of the lowest triplet excited state. The triplets of aryl carbonyls are known as important reactive intermediates in a wide variety of photochemical reactions.[23,26,37−44] Various spectroscopic methods such as ESR,[45−47] nanosecond laser photolysis,[48,49] phosphorescence[26,37−44,50−52] and singlet−triplet absorption,[25,27,53,54] have been utilized to characterize the triplet and correlate with the triplet chemical reactivity. It has been found that, for acetophenone and related derivatives, the lowest $^3n\pi^*$ and $^3\pi\pi^*$ states are so close in energy that the disposition and interaction between the two states are highly sensitive to solvent polarity and the electron donor or withdrawal property of ring substituent groups.[25,26,39−44,48−52] By varying solvent polarity from nonpolar to polar or para-substituted group from electron-withdrawing to donating group, the nature of the triplet state can be varied progressively from a highly reactive $n\pi^*$ configuration to a much reduced reactive $\pi\pi^*$ configuration. Although not many, some time-resolved vibrational spectroscopy studies have been carried out to investigate the possible correlation between the triplet state structure−electronic configuration−reactivity relationship.[55−61] Hamaguchi and co-workers performed TR^3 studies on several aromatic carbonyl compounds possessing typical $n\pi^*$ or $\pi\pi^*$ triplet states.[58−61] They proposed that the frequency of the carbonyl C═O stretching mode in the triplet and its shift from the corresponding ground-state frequency can be taken as a direct indication for the nature of the triplet and can also correlate well with the triplet reactivity.[58−61] However, such vibrational spectroscopy is very scarce compared to the wide and diverse range of other aromatic carbonyl compounds, especially compounds with nearly degenerate $^3n\pi^*$ and $^3\pi\pi^*$ states, as found in the case of acetophenone and its derivatives. The structure and nature of the triplet state of these compounds remain unclear, and it is possible that these triplets could have significantly different properties from those of typical $^3n\pi^*$ and $^3\pi\pi^*$ configurations due to the strongly mixed character of the close-lying $^3n\pi^*$ and $^3\pi\pi^*$ states. It is expected that the work here can begin to contribute to a better understanding of triplet states of this kind.

The TR^3 spectra presented here were acquired with 266 nm excitation and 400 (ps-TR^3) or 416 nm (ns-TR^3) probe wavelength. The triplet lifetime and ISC rate were estimated on the basis of the temporal evolution of the triplet state spectrum recorded by varying the pump and probe time delay from several picoseconds to 400 ns. Density functional theory (DFT) calculations employing the B3LYP method with a 6-311G** basis set have been performed to help determine the triplet structure and vibrational frequencies and to help make assignments to the vibrational bands observed in the experimental spectra. For comparison with the triplet state, the ground-state geometry and vibrational analysis of HPA have also been done at the same level of DFT calculations. We discuss briefly these results in relation to the nature of the triplet state, and the present controversy on the initial stages of the phenacyl deprotection mechanism and related processes.

Experimental and Computational Methods

HPA was synthesized following the method suggested in ref 11. The identity and purity of the sample were confirmed by analysis of NMR, UV absorption, and mass spectroscopic spectra. Spectroscopic grade acetonitrile solvent was used as received for the TR^3 measurements.

A normal Raman spectrum of solid-phase HPA was obtained using a Renishaw Raman microspectrometer employing 514 nm excitation from an Ar ion laser. A FT-IR spectrum of the compound was recorded using a Bio-Rad FTS/64 FT-IR spectrometer with the sample encased in solid KBr windows. The spectral resolutions were approximately 5 cm^{-1} for both the Raman and IR spectra.

Different experimental setups were utilized for the picosecond and nanosecond TR^3 measurements. The picosecond TR^3 experiments were performed using a newly developed ultrafast system in this laboratory. A femtosecond mode-locked Ti:Sapphire laser (Spectra-Physics, Tsunami) pumped by the second harmonic from a Nd:YVO_4 laser (Spectra-Physics, Millennia V) was employed as the seed beam for an amplified laser system. A picosecond mode regenerative amplifier (Spectra-Physics, Spitfire) pumped by the second harmonic from a Nd:YLF laser (Spectra-Physics, Evolution X) amplified the seed laser beam, and the output from the regenerative amplifier (800 nm, 1 ps, 1 kHz) was frequency-doubled and -tripled by KDP crystals to generate the probe (400 nm) and pump (267 nm) laser sources, respectively. The time zero delay between the pump and probe laser beams was found by using fluorescence depletion of *trans*-stilbene, and the time resolution for the TR^3 measurements was determined to be ∼2 ps. The time delay between the pump and probe pulses was controlled using an optical delay line. A recirculated acetonitrile solution with a sample concentration ∼ 1.5 mM was used with the pump and probe beams loosely focused onto a thin film stream (thickness ∼ 500 μm) of the sample solution. Typical pulse energies and spot sizes at the sample for the pump beam were ∼15 μJ and ∼250 μm and the probe beam were ∼8 μJ and ∼150 μm. The Raman light was collected in a backscattering configuration and detected by a liquid nitrogen cooled CCD detector. Each ps-TR^3 spectrum shown here was accumulated over 2 min with

TABLE 1: Structural Parameters of the Ground and Triplet HPA States Calculated from DFT Calculations Using the B3LYP (Ground) and the UB3LYP (Triplet) Methods with a 6-311G Basis Set**

bond length (Å)			bond angle (deg)			dihedral angle (deg)		
	S0	T1		S0	T1		S0	T1
C1−C2	1.382	1.376	C1−C2−C3	119.7	120.2	C1−C2−C3−C4	0.0	0.7
C2−C3	1.401	1.403	C2−C3−C4	120.0	119.6	C2−C3−C4−C5	−0.1	0.5
C3−C4	1.398	1.407	C3−C4−C5	119.8	120.8	C3−C4−C5−C6	0.1	−2.6
C4−C5	1.389	1.379	C4−C5−C6	120.9	120.5	C4−C5−C6−C1	0.0	3.5
C5−C6	1.401	1.427	C5−C6−C1	118.4	117.5	C4−C5−C6−C8	180.0	−178.8
C6−C1	1.405	1.432	C6−C1−C2	121.2	121.3	C5−C6−C8−C9	1.7	15.0
C6−C8	1.488	1.428	C6−C8−C9	117.8	126.7	C5−C6−C8−O11	−178.4	−159.6
C8−C9	1.537	1.497	C5−C6−C8	123.3	123.0	C1−C2−C3−O7	180.0	−179.3
C12−C14	1.504	1.508	C8−C9−O10	110.8	113.2	C4−C3−O7−H19	0.1	−1.1
C9−O10	1.422	1.465	C9−O10−C12	115.9	117.8	C6−C8−C9−O10	176.0	−103.2
C12−O10	1.362	1.350	O10−C12−C14	110.4	110.6	C8−C9−O10−C12	82.3	101.4
C3−O7	1.358	1.361	O10−C12−O13	123.4	124.3	C9−O10−C12−C14	−171.5	−178.8
C8−O11	1.213	1.315	C6−C8−O11	122.2	116.9	C9−O10−C12−O13	8.5	1.4
C12−O13	1.203	1.208	C3−O7−H19	109.7	109.5			
C9−H20	1.092	1.090	C2−C3−O7	117.3	117.7			
C9−H21	1.093	1.089	C8−C9−H20	110.3	109.8			
O7−H19	0.963	0.963	C8−C9−H21	109.7	110.4			
			C9−C8−O11	120.0	116.2			

total energy[a] (hartrees): S_0, −687.9919; T_1, −687.8851

[a] Including Zero Point Energy.

appropriately scaled pump only and probe only spectra being subtracted from a pump−probe spectrum.

Nanosecond-TR^3 measurements were done using an experimental apparatus described previously.[62−64] Briefly, the 266 nm pump wavelength was supplied by the fourth harmonic of a Spectra Physics LAB-170-10 Nd:YAG Q-switched laser. The 416 nm probe wavelength came from the first Stokes of a hydrogen Raman shifted line pumped by the third harmonic (355 nm) from the second Nd:YAG laser (Spectra Physics GCR-150-10). The time delay between the pump and probe beam was changed electronically by a pulse generator, and the time resolution of these experiments was ~10 ns. Excitation energies for the pump and probe pulses were in the 2−2.5 mJ range with a repetition rate of 10 Hz. The arrangements for the sample and Raman signal detection are similar to those used in the picosecond experiments. The measurements were performed under open air as well as under nitrogen and oxygen being bubbled through the sample solution. The accumulation time for each of the ns-TR^3 spectrum was 10 min, and the spectra presented were obtained from subtraction of an appropriately scaled probe-before-pump spectrum from the corresponding pump−probe spectrum. UV absorption measurements before and after sample use revealed no appreciable degradation for both the ns- and ps-TR^3 experiments. Acetonitrile Raman bands were used to calibrate the TR^3 spectra with an estimated accuracy of ±5 cm^{-1} in absolute frequency.

The optimized geometry, vibrational mode, and frequencies for the ground-state HPA were obtained from B3LYP density functional theory (DFT) calculations employing a 6-311G** basis set and C_1 symmetry. The open-shell UB3LYP method with the same basis set was used for the triplet computation. No imaginary frequency modes were observed at any of the optimized structures. The DFT Raman and IR activities were also calculated to allow direct comparison with the experimental spectra. The spin density was obtained from the triplet calculation, and no appreciable spin contamination was found. All the calculations were done using the Gaussian 98 program suite.[65]

Results and Discussion

A. Optimized Structure and Vibrational Analysis of the Ground State of HPA. Figure 1 displays the optimized

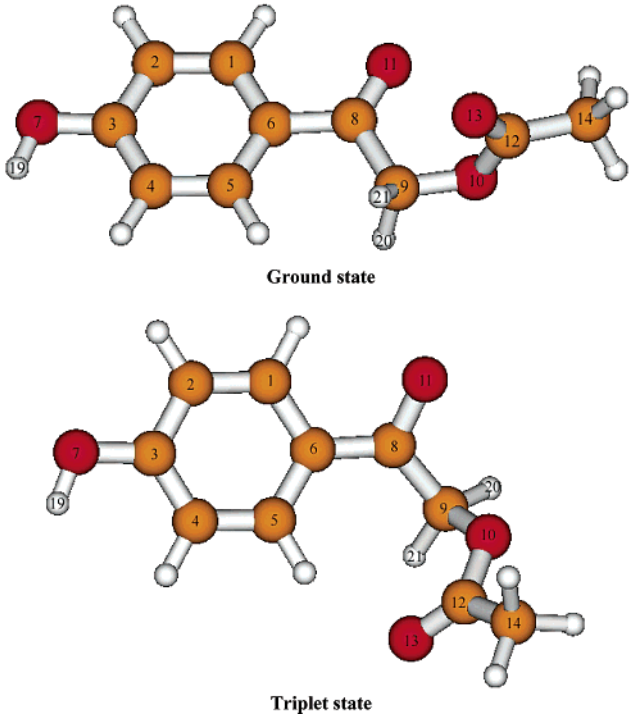

Figure 1. Optimized structure of the ground and triplet states of HPA calculated from DFT calculation using B3LYP (ground) and UB3LYP (triplet) methods with a 6-311G** basis set.

geometry found from B3LYP/6-311G** calculations for the HPA ground state. Selected structural parameters are given in Table 1. Experimental normal Raman and FTIR spectra of HPA in the 400−2000 cm^{-1} region are shown in Figure 2a,c, respectively. Calculated B3LYP/6-31G** Raman and IR spectra based on the optimized structure are presented in Figure 2b,d, respectively, for comparison to the experimental spectra. A Lorentzian function with 10 cm^{-1} bandwidth was used to produce vibrational bands for the calculated spectra in Figure 2. Table 2 provides a summary of the experimental and calculated vibrational frequencies and vibrational assignments made from a direct comparison between the experimental and calculated spectra. The calculated vibrational frequencies were

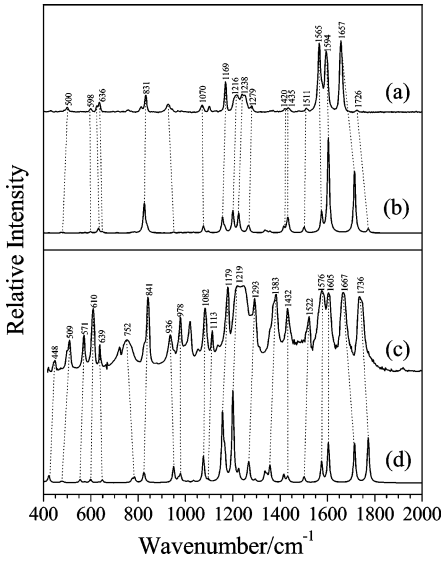

Figure 2. Experimental and DFT calculated normal Raman (a, b) and IR (c, d) spectra in the 400−2000 cm^{-1} region for the ground state of HPA. See text for more details.

scaled by a factor of 0.9718. Vibrational coupling was found to be quite extensive for many vibrational modes, especially for those with contributions from the chain C−C and C−O stretching connecting the acetate moiety to the carbonyl group; the ring-substituted stretching vibration (C6−C8 or C3−O7 stretching) is found to couple substantially with the ring C−C stretching. The assignments are based on the atomic displacements of the calculated normal mode, and the descriptions listed in Table 2 include only vibrations with predominant contributions to the corresponding vibrational modes. When applicable, the Wilson notation is used to label the ring C−H and C−C vibrations analogous to benzene motions.

It can be seen from Figure 1 and Table 1 that, besides H20 and H21, all the other atoms in the *p*-hydroxyacetophenone subgroup and the acetate oxygen (O10) are nearly in the same plane defined by the ring. The plane of the acetate carbonyl O13−C12 and C14 is almost perpendicular to the ring plane as indicated by the ∼82° dihedral angle for C8−C9−O10−C12. The ring is nearly a regular hexagon with the center C−C bond length (∼1.39 Å) slightly shorter than those of the shoulder C−C bonds (∼1.40 Å). The C6−C8 bond connecting the ring and carbonyl has a length (∼1.49 Å) that is moderately shorter than normal C−C single bond length (∼1.52 Å), indicating a certain extent of conjugation between the π systems of the ring and the connecting carbonyl subgroups. The C−O bond connecting the acetate leaving group and the phenacyl "cage" (C9−O10) is longer in length (∼1.42 Å) than those of the other two C−O single bonds (∼1.36 Å for C3−O7 and C12−O10).

To our knowledge, there have been no X-ray diffraction data published for this compound for comparison to the calculated

TABLE 2: Observed and Calculated Vibrational Frequencies (cm^{-1}) and Assignment for the Ground-State HPA (ip, In-Plane; op, Out-of-Plane)

experimental		calculated			
Raman	IR		freq		assigned descriptions
432	448	ν15	422	skeleton deformation	
501	509	ν16	475	skeleton deformation	
		ν17	483	ring C−C and C−H op bending (16b) + CH_2 rocking	
	571	ν18	555	CH_2 rocking + ring C−C and C−H op bending (16b) + C6−C8 op bending	
		ν19	575	C14−C12−O10 op bending + CH_3 wagging	
598	610	ν20	599	ring CCC bending (6a)	
625		ν21	632	ring CCC bending (6b)	
636	639	ν22	648	C12−C14 stretching + ring CCC ip bending (minor)	
714	722	ν23	711	ring C−C and C−H op bending (5)	
a	*b*	ν24	775	C8−C9 stretching + ring C−H ip bending (18a, minor)	
759	752	ν25	784	ring C−H op bending	
812	*a*	ν26	823	ring C−C stretching (6a) + CH_2 and CH_3 rocking	
831	843	ν27	826	ring C−C stretching (6a) + C8−C9 stretching	
		ν28	838	ring C−H op bending + CH_2 and CH_3 rocking	
		ν29	911	ring C−H op bending	
929	936	ν30	950	ring C−C stretching (12) + C8−C9 stretching + CH_3 rocking	
	a	ν31	970	ring C−H op bending + CH_2 rocking (minor)	
983	978	ν32	979	ring C−H op bending + CH_3 and CH_2 rocking	
		ν33	997	ring C−H ip bending (18a)	
998		ν34	1011	CH_2 and CH_3 rocking	
	1019	ν35	1034	CH_3 rocking	
1070	1082	ν36	1076	C9−O10 stretching + CH_3 rocking	
1120	1113	ν37	1097	ring C−H ip bending (18b) + O7−H19 ip bending (minor)	
1169	1179	ν38	1157	ring C−H ip bending (9a) + O7−H19 ip bending	
	b	ν39	1166	O7−H19 bending + ring C−H ip bending (9a)	
1216	1219	ν40	1200	C6−C8 and ν as(O10−C12−C14) + CH_2 wagging + CH_3 umbrella	
1241	*b*	ν41	1225	C6−C8 and ν^{as}(O10−C12−C14) + CH_2 wagging + CH_3 umbrella + ring C−H ip bending (18a)	
1247	1248	ν42	1263	CH_2 twisting	
1279	1297	ν43	1268	C3−O7 stretching + ring C−C stretching + ring C−H ip bending (18a)	
		ν44	1295	ring C−C stretching and C−H ip bending (3)	
1376	1372	ν45	1336	ring C−C stretching (14) + O7−H19 ip bending	
	a	ν46	1344	CH_2 wagging + CH_3 umbrella	
	1383	ν47	1357	CH_3 umbrella + CH_2 scissor	
		ν48	1416	CH_2 scissor	
		ν49	1428	ring C−C stretching (19b) + O7−H19 ip bending	
1420		ν50	1432	CH_3 deformation	
1435	1432	ν51	1435	CH_3 deformation	
1511	1522	ν52	1501	ring C−C stretching (19a) + C6−C8 and C3−O9 stretching	
1565	1576	ν53	1575	ring C−C stretching (8b) + O7−H19 ip stretching	
1594	1605	ν54	1604	ring C−C stretching (8a) + C6−C8 and C3−O7 stretching	
1656	1667	ν55	1715	C8═O11 stretching	
1726	1736	ν56	1773	C12═O13 stretching	

[a] Shoulder bands. [b] Broad bands.

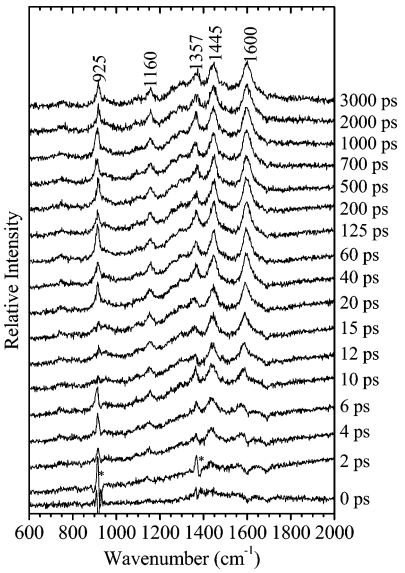

Figure 3. Picosecond time-resolved resonance Raman spectra of HPA in acetonitrile obtained with 266 nm pump and 400 nm probe wavelengths at various time delays that are indicated next to the spectra. The asterisks (*) mark solvent subtraction artifacts.

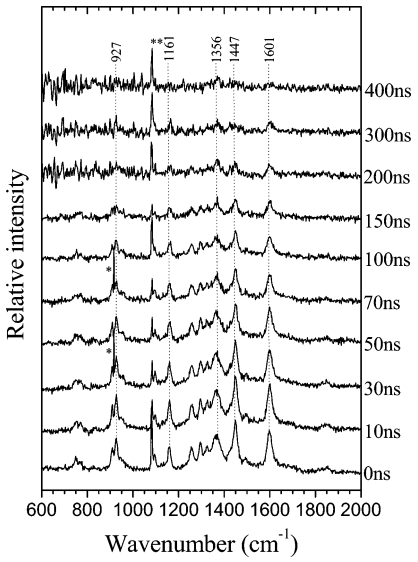

Figure 4. Nanosecond time-resolved resonance Raman spectra of HPA in acetonitrile obtained with 266 nm pump and 416 nm probe wavelengths at various time delays that are indicated next to the spectra. The asterisk (*) marks solvent subtraction artifacts. The double asterisk (**) marks a band due to scattering from the laser line.

geometry. However, inspection of Figure 2 shows that the experimentally observed Raman and IR spectra agree reasonably well with the B3LYP/6-311G** computed spectra. This implies that the optimized structure resulted from the B3LYP/6-311G** computation is reasonable, and this makes assignments of the vibrational bands relatively straightforward. Thus, the carbonyl C═O stretching vibrational modes for both the phenacyl (1657 cm^{-1}) and acetate (1726 cm^{-1}) moieties, and all the other modes can be readily assigned as shown in Table 1. For comparison with the triplet vibrational modes (below), it is necessary to mention here that, although there is a small contribution from the motion of nearby atoms, such as C8−C6/C8−C9 stretching for the phenacyl carbonyl and C12−O10/C12−C14 stretching for the acetate carbonyl stretching motion, the 1657 and 1726 cm^{-1} experimental bands are local in character and dominated by the two C═O stretching vibrations, respectively.

B. Time-Resolved Resonance Raman Spectra. In the TR^3 measurements, the 267 nm pump wavelength lies in the lowest strong UV absorption band of HPA. The large extinction coefficient ($\epsilon = 15\,700$ mol^{-1} cm^{-1}) indicates that the absorption originates from the strongly allowed $\pi\pi^*$ transition of the *p*-hydroxyacetophenone chromphore. The 400 (ps-TR^3) and 416 nm (ns-TR^3) probe wavelengths are within the strong T_1-T_n absorption band (range from ∼300 to ∼480 nm, peaking at ∼400 nm) reported earlier by Wan and co-workers using nanosecond laser photolysis.[11] Figure 3 displays representative ps-TR^3 spectra of HPA in acetonitrile acquired with time delays between the pump and probe pulse that vary from 0 to 3000 ps. The TR^3 spectra obtained on the nanosecond time scale (from 0 to 400 ns) are displayed in Figure 4. The bands observed for the 600−2000 cm^{-1} region are shown in the figures since there were no obvious features recognized below 600 cm^{-1} or in the 2000−3500 cm^{-1} region. With comparison of the spectra shown in Figures 3 and 4, it is clear that spectral features observed on the nanosecond time scale (as listed in Table 3) are the same as those that appear in the later time picosecond spectra (20 ps and afterward). This indicates the same species is detected in both cases. The slight difference in the relative intensity between the picosecond and nanosecond spectra, for example the intensity ratio of the 1447−1601 cm^{-1} band is slightly smaller in the picosecond than nanosecond spectra, can be attributed to the different probe wavelengths used for the respective TR^3 measurements. In addition, due to the transform limit, the bandwidths for features in the picosecond spectra are generally broader than those in the nanosecond ones. Fits to the experimental Raman bands with a Lorentzian band shape found a full width at half-maximum (fwhm) of ∼42 cm^{-1} for the 1601 cm^{-1} band for the late time picosecond spectra but only ∼24 cm^{-1} for the corresponding Raman band in the nanosecond spectra. The better spectral resolution of the nanosecond TR^3 spectra allows features that are overlapped in the picosecond spectra to be resolved clearly in the nanosecond spectra. For example, the three features, 1260, 1298, and 1327 cm^{-1}, are resolved clearly in the nanosecond spectra but appear as an overall broad shoulder band in the picosecond spectra. When the 24 cm^{-1} ns-TR^3 band is convoluted with the 20 cm^{-1} picosecond laser pulse, this results in a band with fwhm = 40 cm^{-1}. This value is very close to the experimental value of ∼42 cm^{-1} for the longer time picosecond spectra. This indicates that the picosecond laser bandwidth convoluted with the intrinsic Raman bandwidth is the main factor responsible for the broadness of the ps-TR^3 bands. This suggests there is no significant saturation broadening due to the probe laser pulse energy.

As shown in Figures 3 and 4, the initial picosecond spectrum (the 0 or 2 ps spectrum) is almost featureless, but it evolves rapidly at very early times and decays in intensity on the nanosecond time scale. By fitting the Raman features with Lorentzain band shapes, Figure 5a displays the time dependence of the 1601 cm^{-1} band areas found from the picosecond spectra. Decays of this band on the nanosecond regime observed under open air, N_2, and O_2 purged conditions are shown in Figure 5b. The kinetics shown in Figure 5 can be fit well by one exponential growth or decay functions for both the pico- and nanosecond time data, and the results obtained by least-squares fits are also displayed in Figure 5. A time constant of 12 ps was found for early time growth (Figure 5a), and 137, 50, and 16 ns were found for the nanosecond decay under N_2 purge, open air, and O_2 purge conditions, respectively (Figure 5b). During the experiments, we found that the nanosecond decay rate increases with increasing sample concentration, and at the

TABLE 3: Observed and Calculated Vibrational Frequencies (cm^{-1}) and Tentative Assignment for the Triplet State HPA (ip, In-Plane; op, Out-of-Plane)

	calculated		
exptl	freq		description
755	ν24	717	C−C stretching (ring + C6−C8)
770	ν25	798	ring C−C stretching (1)
	ν26	801	ring C−H op bending (10a)
	ν27	826	ring C−H op bending (17b)
	ν28	833	ring C9/12−O stretching + C12−C14 stretching
911	ν29	911	C9−O10 stretching + CH_2 rocking + CH_3 rocking
	ν30	949	ring C−H op bending (5)
	ν31	963	ring C−H op bending (17a)
927	ν32	976	C−C stretching (ring, C8−C9) + ring C−H ip bending (18a)
948	ν33	997	CH_2 rocking + ring C−C stretching and C−H ip bending (18a)
948	ν34	1007	ring C−C stretching and C−H ip bending (18a) + CH_2 rocking (minor)
	ν35	1022	CH_3 rocking 0.039 + C9/12−O stretching (minor)
	ν36	1066	CH_3 rocking
1097	ν37	1126	ring C−H ip bending (18b)
1161	ν38	1166	ring C−H ip bending (9a) + C8−C9 stretching
	ν39	1188	O7−H19 ip bending + ring C−H ip bending
1260	ν40	1225	ν^{as}(O10−C12−C14) + ring C−H ip bending (9a) + CH_2 and CH_3 wagging
1260	ν41	1240	ν^{as}(O11−C8−C9) + ν^{as}(O10−C12−C14) + CH_2 and CH_3 wagging + ring C−H ip bending (9a)
1298	ν42	1266	CH_2 twisting + ring C−H ip bending + C6−C8 stretching
	ν43	1299	C3−O7 stretching + ring C−C stretching and C−H ip bending (18a)
1327	ν44	1321	ring C−C stretching and C−H ip bending + C3−O7 stretching
1356	ν45	1366	C6−C8 stretching + ring C−C stretching and C−H ip bending + O7−H19 ip bending
1356	ν46	1372	C6−C8 stretching + O7−H19 ip bending + minor ring C−C stretching and C−H ip bending
	ν47	1376	CH_2 rocking + CH_3 umbrella
	ν48	1401	CH_3 umbrella + CH_2 rocking
1447	ν49	1455	ring C−C stretching + CH_2 scissor
	ν50	1466	CH_2 scissor (major) + ring C−C stretching (minor)
	ν51	1472	CH_3 deformation
	ν52	1476	CH_3 deformation
	ν53	1505	ring C−C stretching (19a) + C6−C8 stretching + CH_2 scissor
1493	ν54	1548	ring C−C stretching (8b)
1601	ν55	1580	ring C−C stretching (8a) + C3−O7 stretching
	ν56	1793	C═O13 stretching

same time, Raman bands due to an additional new species were detected at the expense of the Raman features shown in Figure 4. Such concentration dependence has been observed in closely related compounds, such as *p*-hydroxyphenacyl diethyl phosphate[8] and *p*-hydroxypropiophenone,[66] and can be attributed to a self-quenching effect due to head-to-tail hydrogen abstraction leading to the radical-derived photoproducts produced even in specially dried acetonitrile.

The observation that the lifetime of the intermediate decreases significantly in the presence of oxygen and approaches the diffusion limit under oxygen-saturated condition suggests it is triplet in nature, and this is consistent with previously reported results of Wan and co-workers[11] and Givens and co-workers.[5,7,8] However, we note that the lifetime we obtained here under N_2-purged condition (137 ns) is noticeably shorter than the 1.1 μs lifetime reported by Wan and co-workers and could be due to some trace amounts of oxygen still being present in our sample (see later part of paragraph).[11] To verify further the triplet assignment, we have recently carried out femtosecond Kerr-gated time-resolved fluorescence measurement on this compound. This experiment was done with 266 nm excitation in acetonitrile, and a ~2 ps time constant was obtained from the measured fluorescence decay. This implies that ISC conversion from the singlet to triplet occurs with a rate of $\sim 5 \times 10^{11}$ s^{-1}.[67] This HPA ISC rate is similar to the 2.7×10^{11} and $(3.8 \pm 0.2) \times 10^{11}$ s^{-1} ISC rate reported for the closely related compound *p*-hydroxyacetophenone and *p*-hydroxyphenacyl diethyl phosphate, respectively.[8] This correlates with the rapid growth of the TR^3 spectrum in the early picosecond time regime and provides additional confirmation that the intermediate we observed is indeed from the triplet state of HPA. The result is consistent with the general view that aryl carbonyl compounds have high ISC yields with rapid ISC rates. For example, Wagner and co-workers reported that the ISC yield of methoxy ketones are nearly unity in polar and nonpolar solvents.[26] Similarly, Rentzepis reported that the ISC rate of benzophenone is ~0.5−15 ps, depending on the excitation wavelength.[24] We think the 1.1 μs triplet lifetime obtained by Wan and co-workers (using a degassed enclosed sample) is a better estimate of the actual triplet lifetime in the absence of oxygen. We attribute our shorter 137 ns lifetime as being due to the degassing method used in our experiment that is not efficient enough to reduce the concentration of residual oxygen to a small enough value to get a very accurate lifetime of the triplet in the absence of oxygen. According to the measured triplet lifetimes and taking the pseudo-unimolecular oxygen quenching rate as $\sim 10^{10}$ M^{-1} s^{-1}, the oxygen concentration in the solution can be estimated to be $\sim 7.3 \times 10^{-4}$, 2×10^{-3}, and 6.25×10^{-3} M under the nitrogen-purge, open-air, and oxygen-purge conditions, respectively. This indicates that, by bubbling nitrogen through the open circulated-solution system, we can remove ~65% oxygen from the solution and the residual 35% can account for the shorter lifetime found here.

It is important to point out that the ~2 ps fluorescence decay does not match exactly with the ~12 ps growth of the triplet spectrum. Therefore, besides the ISC conversion, there must be some other process responsible for the development of the triplet TR^3 spectra at very early picosecond times, and we attribute this to the triplet relaxation of excess energy from the rapid ISC conversion and formation of an unrelaxed triplet state. By checking the fitting result of the picosecond spectra at different time delays, we found that the band frequency shows some upshift on a time scale similar to that for the growth of the intensity of the triplet state Raman bands. Figure 5c displays the temporal change for frequency of the ~1601 cm^{-1} band up to 200 ps. It can be seen that frequency of the band shifts by

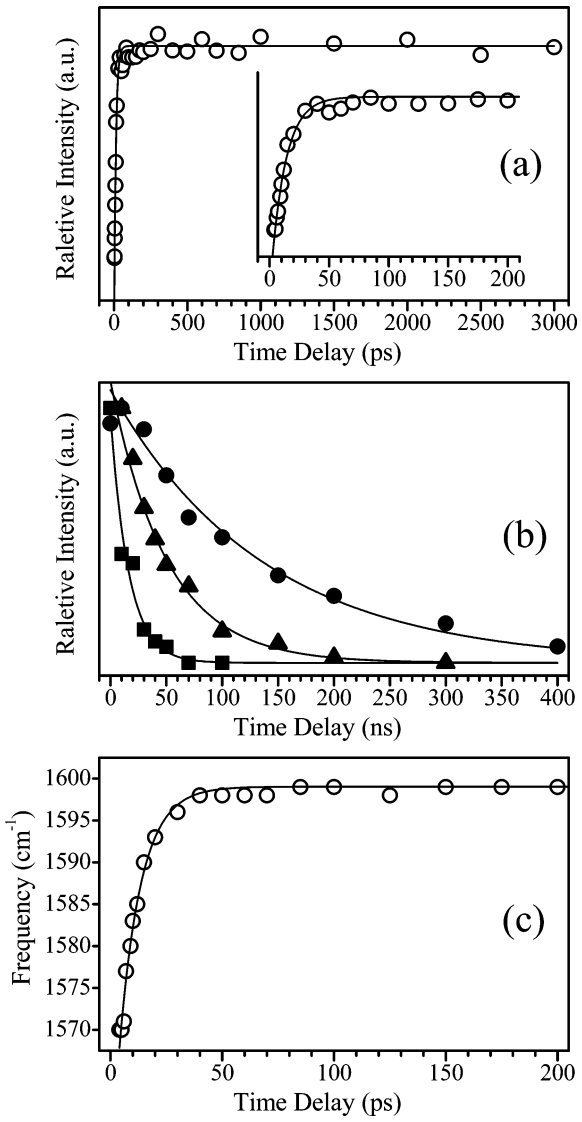

Figure 5. (a) Time dependence of the triplet 1601 cm^{-1} band areas in the ps-TR^3 spectra shown in Figure 3 (open circles). (b) Time dependence of the triplet 1600 cm^{-1} band areas the in ns-TR^3 spectra under nitrogen purge (filled circles), open air (filled triangle), and oxygen purge (filled square) conditions. Solid lines are results of fits to the data (see text). The insert in a gives details of the early time kinetics. (c) Time dependence of the triplet ~1601 cm^{-1} band frequency in the ps-TR^3 spectra shown in Figure 3 (see text for details).

~31 cm^{-1} from 1570 cm^{-1} at 4 ps to 1601 cm^{-1} at 50 ps and afterward. The temporal change can be fitted by one exponential with a ~10 ps time constant, which matches very well with the 12 ps found from the intensity change of the Raman bands. We note that the band also shows narrowing in width within this time scale. All of these indicate that the excess energy relaxation process is the main factor to account for the observed early time spectral evolution. It has been reported for several molecules that relaxation of excess energy produces band changes of such as those observed here in the TR^3 spectra on a very similar time scale.[68−72] The availability of this excess energy implies that the lowest triplet of HPA is substantially lower in energy than the singlet. The energy separation between the ^{1}nπ^* and ^{3}nπ^* states was estimated to be ~1800 cm^{-1} for acetophenone[25,53] and that between ^{3}nπ^* and $^3\pi\pi^*$ to be ~2500 cm^{-1} for *p*-hydroxyacetophenone.[54] With the $^1\pi\pi^*$ and ^{1}nπ^* being close in energy as indicated by HPA ground-state UV absorption spectrum, this could be taken as a hint for the energy of the $\pi\pi^*$ triplet of HPA.

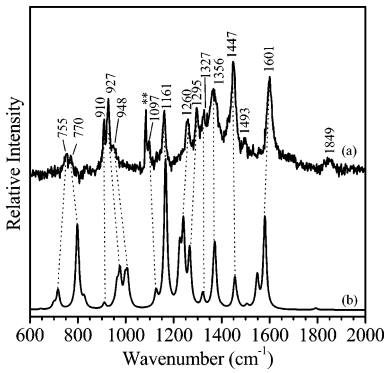

Figure 6. Comparison of the experimental resonance Raman spectrum of the HPA triplet (a) with the DFT-calculated triplet Raman spectrum (b). The double asterisk (**) marks a band due to scattering from the laser line.

The possibility that the 12 ps early time process is due to the excited-state deprotonation of HPA phenolic proton can be ruled out based on the following: (i) the deprotonation occurs only in water-involved solvent,[8,10,11] whereas the spectra presented in Figure 3 are recorded from pure acetonitrile; (ii) the transient species produced from the possible deprotonation and related processes have been reported to absorb in the 300−380 nm range for photoexcited HPA[11] and therefore will not be resonantly enhanced with the 400 nm probe wavelength used here for the ps-TR^3 measurement; (iii) The excited-state deprotonation has been found to occur with a rate of ~9 × 10^6 s^{-1} for the parent compound *p*-hydroxyacetophenone in aqueous acetonitrile (50% H_2O).[8] In general agreement with this, our preliminary ps-TR^3 experiment for HPA in aqueous acetonitrile showed that the deprotonation-related reactions of photoexcited HPA take place with time constants on the nanosecond time scale,[67] too slow to be responsible for the ~ 12 ps early time process.

We note that experimental evidence for the coexistence of two triplets has been presented in the literature for some aromatic carbonyls with close-lying nπ^* and $\pi\pi^*$ triplet states.[26,40,61] To check the situation for the HPA triplet, we have done the TR^3 measurement using different probe wavelengths (341, 355, 400, and 416 nm) spanning the T_n-T_1 absorption bands.[11] The spectra acquired at different probe wavelengths show small differences in their spectral profile, but most of the obvious features appear at the same frequencies. This corroborates and is consistent with the observation that the spectra in all of these cases show the same single-exponential nanosecond decay as that found for the 416 nm spectra presented earlier and indicates that only one triplet is detected.

C. Structure of the Triplet State. To characterize the triplet and make assignment to the triplet TR^3 spectrum, we present here optimized structure, vibrational frequency, and Raman intensities obtained from DFT UB3LYP/6-311G** computations. The calculated geometry and relevant structural parameters are given in Figure 1 and Table 1, respectively, for comparison with the corresponding ground state results. In Table 1, we also listed the calculated total energies including the zero-point energies for both the triplet and ground states, from which a 67.0 kcal/mol triplet energy can be calculated. This triplet energy is in good agreement with an experimental value of 69−71 kcal/mol triplet energy reported from phosphorescence measurements for a *p*-hydroxyphenacyl chromophore.[6,8] Figure 6 displays comparison between the experimental (the 10 ns spectrum shown in Figure 4) and calculated triplet spectra. No scale factor was used for the calculated spectrum. It can be seen that the calculation reproduces reasonably well the experimental spec-

trum. The differences in relative intensities among various features between the experimental and calculated spectra are within expectations since the former is obtained with resonance enhancement while the latter corresponds to a normal Raman spectrum for the triplet. Preliminary assignments have been made straightforwardly on the basis of the correlation between the two spectra. The observed triplet band frequencies together with corresponding computed values and their tentative assignments are summarized in Table 3.

Most experimental bands are calculated to be from vibrations of the phenacyl subgroup. Most features are dominated by phenyl ring related vibrations: the 1601, 1493, 1447, 1327, 770, and 755 cm^{-1} features are mainly due to various ring C−C stretching vibrations; the 1161, 1097, and 927 cm^{-1} bands are predominately from various ring C−H in-plane bending motions coupled differently with ring C−C stretching vibrations. The 1298 cm^{-1} feature, though dominated by the CH_2 twisting, couples strongly with ring C−C and C−H vibrations. According to the calculation, only the 911 cm^{-1} experimental feature is dominated by C9−O10 stretching vibration, the motion leading to cleavage of the acetate from the phenacyl "cage". It is unlikely that we can assign the weak experimental feature at 1849 cm^{-1} to the acetate carbonyl C═O stretch mode calculated to be at 1793 cm^{-1}. This is because of the following: (i) We have recently obtained a similar triplet TR[3] spectrum for *p*-hydroxyacetophenone, a compound closely related to HPA but without the acetate group where we have observed a similar weak band at ∼1840 cm^{-1}. (ii) The calculation shows that the conformation of the acetate moiety remains almost unchanged from the ground to the triplet state so that there is no expectation for any obvious change in frequency of the acetate carbonyl CO stretch that was found to be at 1726 cm^{-1} in the ground state (Table 2). We therefore make a preliminary assignment of the 1849 cm^{-1} band to overtone of the 927 cm^{-1}.

It is important to identify the ring-attached carbonyl CO stretching mode in the triplet state since it can help to establish the nature of the triplet for aromatic carbonyls.[55,57−60] Two experimental features 1356 and 1260 cm^{-1} are found to have contributions from vibrations of the ring-attached carbonyl group. They are correlated with calculated bands of nearby frequencies 1366, 1372 cm^{-1} and 1240, 1225 cm^{-1}, respectively. The calculation indicates that, unlike the case in the ground state (1656 cm^{-1}), there is no localized CO stretching in the triplet and the four carbonyl-related features are all found to be strongly mixed modes. To help make a more unambiguous assignment to mode(s) with the most contribution from the CO stretching vibration, we have preformed DFT frequency and intensity calculations for the carbonyl ^{13}C and ^{18}O isotopically substituted HPA, respectively, for both the triplet and ground states. The 1366 and 1372 cm^{-1} calculation features, corresponding to the 1356 cm^{-1} experimental band, show hardly any isotopic shift upon ^{18}O substitution but shift by ∼20 cm^{-1} upon ^{13}C substitution. The modes therefore have a minor contribution from the CO stretching and are dominated by the ring−carbonyl stretching (C6−C8) coupled with ring C−C and C−H vibrations (see Table 3)

The calculated features 1225 and 1240 cm^{-1}, attributed to the 1260 cm^{-1} experimental band, show a frequency downshift upon ^{18}O substitution by 7 and 4 cm^{-1}, respectively. Frequencies of these two modes also shift down by 12 and 5 cm^{-1}, respectively, upon ^{13}C substitution. This indicates that the modes indeed have a contribution from the carbonyl CO stretching. However, we note that the extent of the isotopic shift is far too small compared with the value for the localized carbonyl CO stretching vibration. For example, the frequency was calculated to shift down by ∼33 and 40 cm^{-1} upon the ^{18}O and ^{13}C isotopic substitution, respectively, in the ground state of HPA; an ∼24 cm^{-1} downshift upon ^{18}O substitute has been reported for localized CO stretching in the $\pi\pi^*$ triplet of fluorenone.[55] The small isotopic shifts observed for the HPA triplet in the DFT calculations can be taken as a reflection of the vibrational mixing character for this vibration. Checking the atom displacements indicates that both calculated modes can be described by an antisymmetric stretching of ring-attached carbonyl C8, ν^{as}(O11−C8−C9), coupled substantially with the antisymmetric stretching of the acetate carbonyl C12, ν^{as}(O10−C12−C14). The ν^{as}(O11−C8−C9) motion includes the carbonyl stretching C8−O11. We note that mode mixing of the triplet CO stretching with other vibrations has been pointed out for both $^3n\pi^*$ and $^3\pi\pi^*$ triplets of aromatic carbonyl based also on small ^{18}O and ^{13}C isotopic shifts.[58,59,61] From the general view that modes having closer frequencies mix more efficiently and the fact that bonds connecting O10−C12, C12−C14, and C8−C10 are all single bond in character, it is expected that the pure carbonyl CO frequency in the triplet is also in the single-bond frequency region around 1200−1300 cm^{-1}. Since the ground CO stretching frequency is 1656 cm^{-1}, this implies a striking frequency downshift (more than 300 cm^{-1}), thus a significant weakening of the carbonyl CO bond upon the triplet formation.

The calculations show that most vibrational modes in the triplet state are not analogous to those of the ground state. However, to better understand the properties of the triplet state, it is still instructive to compare the frequencies of the vibrational modes in the triplet and ground states that have predominantly similar character. Representative examples are as follows. The frequency of modes dominated by the phenyl ring center C−C stretching (the Wilson 8a) and the C−H in-plane bending (the Wilson 9a) show little change in the triplet (1601, 1161 cm^{-1}) from ground-state values (1594, 1169 cm^{-1}). Vibrations with contributions mostly from ring shoulder C−C stretching shift down from 1565 cm^{-1} in the ground to 1493 cm^{-1} in the triplet. This implies that the ring shoulder C−C bond becomes weaker while the center C−C bond remains the same on going from the ground to the triplet state. The frequency of the mode dominated by stretching of the ring-carbonyl (C6−C8) increases from ∼1240 cm^{-1} in the ground to 1356 cm^{-1} in the triplet state, indicating the corresponding bond gains significant double bond character in the triplet state.

The frequency and expected structural changes from the ground to the triplet state are consistent with the calculated structures of the two states, as given in Figure 1 and Table 1. For example, the bond length of the ring center C−C shows little change but the shoulder C−C bonds near the carbonyl (C1−C6 and C5−C6 bond) lengthen by ∼0.03 Å on going from the ground to the triplet state. Compared with the ground state, the carbonyl C8−O11 bond lengthens by ∼0.1 Å and the C8−C6 bond connecting the carbonyl and ring shortens by ∼0.06 Å in the triplet. The bond length of the ring-attached carbonyl (∼1.32 Å) is similar to the length of the C12−O10 single bond in the acetate group (∼1.35 Å) and agrees fully with the single-bond character of the carbonyl group in the triplet as inferred in the preceding discussion. Besides the variations in bond lengths, the conformational change in the triplet involves the relative orientations between the ring and connected carbonyl group and between the phenacyl and acetate moieties. In the ground state, the ring-attached carbonyl, nearby C9, and the acetate oxygen O10 are all nearly in the ring plane. While in the triplet state, the plane constituted by the carbonyl and C9

twists out of the ring plane by ~20°, and the O10 derivates significantly from the ring plane as indicated by the change of the C6−C8−C9−O10 dihedral angle from 176° in the ground to −103° in the triplet state. Accompanying these orientation changes, the C8−C9 bond of the phenacyl group shortens by ~0.04 Å and the C9−O10 bond connecting the phenacyl and acetate groups lengthens by ~0.05 Å. Structural parameters related to the acetate subgroup stay almost unchanged in the triplet compared to the ground state. The bond angle showing the most change is the ring carbonyl related C6−C8−C9 angle that increases slightly from the ground (118°) to the triplet (127°), but the carbonyl C8 atom keeps its planar sp^2 character in both states as indicated by the ~360° sum of angles around C8 (Table 1). The structural change in the triplet state has some implications in the discussion of the nature of the triplet state and the deprotection mechanism.

D. Nature of the Triplet State. There has been extensive experimental evidence that the lowest nπ^* and $\pi\pi^*$ triplet states of acetophenone are nearly degenerate.[25−27,39−44,48,50−54] Consequently, the nature of the lowest triplet is highly sensitive to external perturbations such as substituent groups, the phase or medium (crystal, solvent, or gas phase), solvent polarity, and temperature, etc. For example, the lowest triplet of acetophenone has been attributed to be mainly nπ^* in nature in the gas phase[25] and in nonpolar solvents[48,54] but $\pi\pi^*$ in nature in polar solvents and in the crystalline phase.[48,50−53] Most para-substituted acetophenone derivatives have been suggested to possess a lowest triplet of $\pi\pi^*$ origin in both nonpolar and polar solvents.[48−54] Using low-temperature phosphorescence and phosphorescence excitation spectroscopy, the nπ^* and $\pi\pi^*$ triplets have been found to couple with each other vibronically by effective out-of-plane mode such as the twisting of the $COCH_3$ group.[25,50−54] It has been proposed that the conformation of the carbonyl group, including the bond length and relative orientation between the carbonyl and the phenyl ring, changes significantly from the ground to the triplet state in either the nπ^* or $\pi\pi^*$ character triplet state.

The present TR^3 measurement revealed that the triplet spectrum of HPA resembles the triplet spectrum of *p*-hydroxyacetophenone closely indicating that chromophores responsible for the Raman excitation and most of the important structural features of the triplet are nearly the same in the two compounds. We therefore expect a similar triplet nature for the phenacyl compound to that of *p*-hydroxyacetophenone. On the basis of the band position, the phosphorescence profile, and the lifetime, it has been suggested that the triplet of *p*-hydroxyacetophenone is $\pi\pi^*$ in character[26,54] and we infer the same triplet disposition to HPA. This assignment and the triplet conformation as presented above can be well-understood in terms of ample information for the triplet of acetophenone and derivatives presented in the literature.

It is expected that, for a $\pi\pi^*$ transition, an electron is exited from the highest occupied π orbital to the lowest unoccupied π^* orbital. Our DFT-calculated MO result is consistent with this. The calculation shows that both the bonding and antibonding molecular orbital have contributions from the ring π system and carbonyl π orbital with the bonding π orbital residing more on the benzene ring and antibonding π^* more on the carbonyl orbital. Thus, this $\pi\pi^*$ transition leads to a reduction of electron density in the bonding π orbital and at the same time an increased electron density in the antibonding π^* orbital that results consequently in geometrical change in the related subgroups. This provides an explanation for the observed frequency downshifts of the ring CC and carbonyl CO stretching vibrations and the corresponding geometry change on going from the ground to the triplet state. Reduction of the carbonyl CO double bond strength is expected to be striking due to the simultaneous decrease of the π bonding electron density and the increase of the π^* antibonding density.

As mentioned above, in the triplet state the ring-connected carbonyl twists out from the ring plane by ~15° and the orientation of the acetate with respect to the phenacyl subgroup also changes substantially from the ground-state structure. It is conceivable that these changes can be achieved by a torsional motion of the $-C(O)CH_2-$ group and rotation of the $-CH_2O-$ group about the C8−C9 axis, respectively. In most cases, a planar structure is expected in a pure $\pi\pi^*$ excited state for an aromatic molecule with a planar ground-state conformation. Thus, we attribute the twisted conformation to be caused by vibrational coupling with the nearby high-lying nπ^* triplet, as is the case for the triplet state of acetophenone. The electron-donating hydroxy group substituent induces a wider nπ^* and $\pi\pi^*$ triplet energy gap than that in acetophenone, but the gap is still close enough for efficient vibrational coupling though the extent of couple is not as extensive as in the case of acetophone.[25,26,39,41,43,44,48,50−54] The torsional vibration of the $-C(O)-CH_3$ and the rotation of the $-CH_3$ around the CC axis have been identified as effective out-of-plane modes coupling the closely spaced nπ^* and $\pi\pi^*$ states for the acetophenone triplet and this coupling results in large conformational changes along these two coordinates for the lowest triplet of acetophenone.[25,50−54] It is therefore reasonable to suggest the same effect occurs to some extent for the triplet of *p*-hydroxy-substituted acetophenone derivatives.

To check the reactivity of the HPA triplet, we have recently carried out TR^3 measurement for HPA in 2-propanol solvent with the same pump and probe wavelengths as those used here in the nanosecond TR^3 experiments. We found that the triplet lifetime is about the same as that observed in acetonitrile solvent (Figure 4, 5b). Since 2-propanol is an efficient H-atom donor solvent, this observation implies that the HPA triplet has fairly low reactivity toward the hydrogen abstraction reaction. This is consistent with the low reactivity of the $\pi\pi^*$ triplet for *p*-hydroxyacetophenone as reported in the literature.[26,38,41,44,53,54] On the other hand, for a triplet of nπ^* nature, a high hydrogen abstraction reactivity is expected due to electron deficiency of the carbonyl oxygen.[38,41,44,49] Therefore, the observation of very similar lifetimes in both acetonitrile and 2-propanol solvents supports the $\pi\pi^*$ character we have assigned to the HPA triplet.

E. Initial Step for the Phenacyl Photodeprotection Reaction. It has been shown that, in acetonitrile, photoexcitation of phenacyl compounds including the various phenacyl-caged biological stimulants leads to solely the formation and decay of the corresponding triplets;[8,11] whereas the deprotection and rearrangement process occurs in water-mixed acetonitrile or aqueous solution.[2−11] Our assignment here of the triplet for HPA in acetonitrile is consistent with those of previous suggestions from Givens and co-workers[8] and Wan and co-workers[11] In terms of kinetic analysis, one important result of the present work is the rapid formation of the HPA triplet with the ISC conversion rate estimated to be ~2 ps. Although the work is not done in a water-involved environment, these results enable us to make some comments on the ongoing controversy about the mechanism of the phenacyl photodeprotection reaction. As cited in the Introduction, one major argument is the issue of multiplicity: Givens and co-workers proposed the photorelease process occurs from the phenacyl triplet,[2−9] whereas Wan and co-workers emphasized the initial step is the ESIPT origin from

the phenacyl singlet state.[10,11] The result reported here implies that, to compete effectively with the rapid ISC process, the singlet-state intramolecular proton transfer must occur with a sub-picosecond time constant. Although there have been examples that both direct inter- or intramolecular proton transfers can occur in sub-picosecond and even femtosecond time scales,[28−36] this appears somewhat unlikely for the phenacyl proton transfer since, rather than a direct proton transfer between the donor and acceptor, the suggested ESIPT mechanism is a kind of water-mediated process between the well-space-separated proton donor (the −OH group) and acceptor (the ketone oxygen atom).[10,11] It is conceivable that a suitably located and orientated water cluster composing several water molecules is required for such a mediated process to occur. The cluster formation requires translation and rotation of the involved water molecules that makes the proton transfer take place on a slower time scale and consequently may not be efficient enough to compete with the very efficient ISC conversion process. This is especially true since the HPA photodeprotection has been observed to occur at low water concentration such as 5% (v:v) water in acetonitrile. In this regard, our result would tend to favor the view that the triplet is the reactive intermediate to the subsequent photorelease reaction. Further ultrafast experiments comparing our present results in acetonitrile to those in water and/or water/acetonitrile solvents should prove useful in obtaining a more definitive answer to the multiplicity of the state or states leading to the deprotection reaction.

In terms of the cleavage pathway of photoexcited HPA, our present results indicate the *p*-hydroxyphenacyl moiety is the chromophore responsible for photoexcitation. The major geometric change in the triplet is also at the *p*-hydroxyphenacyl group, and this implies that further energy transfer from the phenacyl triplet to the leaving group accompanied by some conformational modification is required for the cleavage to occur. Givens and co-workers favor a cleavage mechanism involving direct release of the leaving group (the acetate moiety here) from the excited triplet[3−9] and put forward two possible pathways: (i) transfer of the π^* electron of the phenacyl moiety to the σ^* orbital of the $-CH_2-O-$ bond (corresponding to the C9−O10 bond here);[3,5,6] (ii) homolytic fragmentation of the $-CH_2-O-$ bond followed by rapid electron transfer.[5,9] Our DFT calculations found that the C−O (C9−O10 in the molecule studied here) bond connecting the phenacyl and acetate group shows a noticeable but small lengthening by 0.043 Å on going from the ground (1.422 Å) to the triplet state (1.465 Å); the relative orientation of the acetate to the phenacyl subgroup also changes from the ground to the triplet state due to rotation of the C8−C9 (rather than the C9−O10) bond, whereas conformational parameters of the acetate moiety remain almost unchanged between the two states. This result appears to lend little direct support to the direct triplet cleavage argument but nevertheless is consistent with the experimental fact that the photoinduced deprotection reaction does not take place in pure acetonitrile where the triplet is the dominant reactive intermediate.[8−12] This, on the other hand, also implies that water, as solvent, must play a crucial role for the deprotection process to occur. Plausible mechanisms of this kind could be a triplet proton transfer[8,10,11] or water catalysis by solvation of the leaving group to drive its dissociation into ions.[73] In addition, the lack of triplet reactivity toward hydrogen abstraction implies that the hydrogen abstract path suggested by Falvey and co-workers[12] may not be applicable to the photodeprotection of the HPA system, although the hydrogen abstraction pathway provides a good explanation for the photorelease process of an unsubstituted phenacyl acetate. Further time-resolved experiments and theoretical calculations considering explicitly the role of water are planned to better address what happens to the photoexcited *p*-hydroxyphenacyl-caged compounds in aqueous and/or mixed aqueous systems.

F. Comparison with Previous Time-Resolved Vibrational Spectroscopy Results for Other Aromatic Carbonyl Compounds. To our knowledge, the spectra given here are the first TR^3 spectroscopic study reported for hydroxyphenacyl esters. We also present the first computed-optimized structure for the triplet state of HPA. The only other time-resolved vibrational spectroscopy on acetophenone-related compounds is a TRIR study by Toscano and co-workers on the triplet of *p*-methoxyacetonphenone and *p*-trifluoromethyacetophenone.[56] There are also several TR^3 and TRIR works performed on the triplets of aryl ketones such as benzophenone,[59,60] 4-phenylbenzophenone,[58,74] fluorenone,[55] duroquinone,[57] 2-naphthaldehyde,[61] and related compounds.[75] It is worthwhile to compare and discuss our results in relation to these previous studies.

The carbonyl CO stretching in the triplet state has received the most attention since it helps to characterize the nature and properties of the triplet. For its identification, isotopic substituted derivatives (especially the carbonyl ^{18}O and/or ^{13}C labeled samples) have been used in some experiments.[55−60,74] There are generally two different observations found from these previous studies. In one class of observations, the CO stretching mode can be identified experimentally and it was found to appear in the 1500−1610 cm^{-1} range for $\pi\pi^*$ triplet states and in the 1200−1400 cm^{-1} region for $n\pi^*$ triplet states. In this class of observations, it has been proposed that the CO frequency can be regarded as a direct indicator for the nature of the triplet state.[55,57−60,74] In the second class of observations, the CO stretching mode cannot be unambiguously identified experimentally due to either its absence[61,75] in the experimental spectra or a lack of observation of the expected isotopic shift.[56] The absence of the experimental band from this mode was also noted in phosphorescence excitation spectroscopy for acetophenone derivatives.[25,53] This has been interpreted as being due to a decrease in the CO frequency and a strong mixing of this mode with other modes so that the CO stretching does not exist as a separate normal mode and any intensity previously associated with a single pure CO stretching mode becomes distributed among the several other modes. We note that even in examples of the first class of observations where distinct CO stretch modes are observed such as the $n\pi^*$ triplet of benzophenone (1222 cm^{-1}) and the $\pi\pi^*$ triplet of 4-phenylbenzophenone (1522 cm^{-1}), the vibrational mixing of this mode with other modes is noticeable. This can account for the observed extent of the ^{18}O and ^{13}C isotopic shifts being noticeably less than those expected for a pure CO stretch mode.[58−60] Exceptions for the vibraional mixing are the $\pi\pi^*$ triplets of flourenone[55] and duroquinone[57] in which the CO stretching shows the expected isotopic shift in the TRIR spectra. It is possible that this is due to a lack of flexibility for carbonyl conformational relaxation in the excited state because, in both compounds, the carbonyl group is sterically hindered and almost fixed in the ring plane.

Our results here for the triplet of HPA is that there is no localized ring-attached carbonyl CO stretching mode; our tentative assignment suggests it mixes with single-bond character CO (C12−C10) stretching of the acetate subgroup. This is consistent with the vibrational mixing character of the CO stretching as reported in several previous studies.[25,53,58−61] It is possible that loss of the CO vibration as a unique normal mode in the triplet state is a general phenomenon with aryl carbonyl

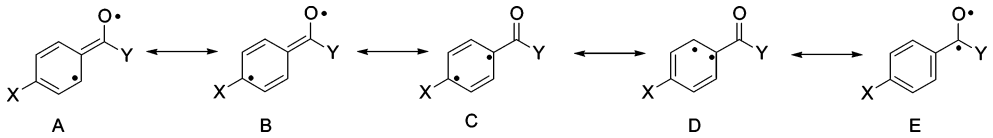

Figure 7. Major resonance contributions for the nπ^* and $\pi\pi^*$ triplets of para-substituted aromatic carbonyl compounds.

TABLE 4: Spin Density Distribution for the Triplet HPA Obtained from the DFT UB3LYP/6-311G Calculation**

ρC1	0.206	ρC8	0.453
ρC2	−0.101	ρC9	0.039
ρC3	0.243	ρO10	0.031
ρC4	−0.065	ρO11	0.904
ρC5	0.190	ρC12	−0.001
ρC6	0.032	ρO13	0.003
ρC7	0.062	ρC14	0.002

compounds possessing a flexible carbonyl group though more examples need to be studied to see if this is generally the case.

We note that our assignment is not quite in line with the previously suggested correlation between the triplet nature and the carbonyl CO stretching frequency. As illustrated above, we estimated frequency of the HPA triplet CO stretching is in the 1200−1300 cm^{-1} region, and we assigned the triplet as $\pi\pi^*$ in nature. According to previous predictions, a triplet with a CO frequency in 1200−1300 cm^{-1} is expected to be predominately nπ^* nature, rather than the $\pi\pi^*$ character.[55,57−60,74] The divergence from this characterization must stem from the different electronic properties between the compound studied here and those examined in previous work and can be understood in the following way. It is generally known that the electronic distribution in a triplet of aromatic carbonyl compound depends highly on the nature and position of the substituents.[25,26,39−54] When the phenyl ring is substituted by an electron donating group such as hydroxy at a para-position to the carbonyl moiety, the energy of ring-dominated π orbitals increase. This in turn leads to (i) a lowering of the energy for a $\pi\pi^*$ transition and a raising of the energy for an nπ^* transition (ii) and a change of the mixing between the carbonyl π and π^* orbitals with those of the phenyl ring.[26,44,48,52−54] Experimental indications for i are the significant bathochromical shift of the strong $\pi\pi^*$ UV absorption band (L_a type) in the substituted carbonyls compared with nonsubstituted carbonyls[26,52−54,76,77] and the reversal of the nπ^* and $\pi\pi^*$ triplets between the substituted and nonsubstituted compounds.[26,48,52−54] For example, the steady-state absorption spectrum of HPA in acetonitrile indicates that the L_a absorption maximum at ∼270 nm shifts to the red by 30 nm from that of acetophenone, which has a maximum at ∼240 nm. The shift makes the two lower energy weak bands (the $\pi\pi^*$ L_b type and nπ^* transitions) in HPA become completely buried under the intense L_a band, while the L_b and nπ^* bands can be discerned clearly at ∼280 and ∼290 nm, respectively, for acetophenone. The reversals of the nπ^* and $\pi\pi^*$ triplets are due to the $\pi\pi^*$ triplet being correlated electronically with the L_a transition.[26] Experimental evidence for ii is the triplet EPR measurement showing a sharp reduction in the D value from nonsubstituted aromatic carbonyls compared to para-substituted aryl ketones. This was interpreted as a reflection of the delocalization of the free spin onto the carbonyl group that has been taken to account for intrinsic reactivity of lowest $\pi\pi^*$ triplets for some aromatic ketones.[26,45−47] As given in Table 4, the spin density found from our triplet DFT calculation is consistent with this. It can be seen that the free spin distributes mainly on the carbonyl oxygen and carbon atoms with some amount on the three carbon atoms of the ring.

In this regard, it is appropriate to mention the classical notations concerning the nπ^* and $\pi\pi^*$ triplet as represented by the resonance structures shown in Figure 7. For the $\pi\pi^*$ triplet, the bonding changes of the molecule are expected to be throughout the entire system as described by the resonance forms A−D, while for a typical nπ^* triplet (where the nonbonding orbital is localized on the carbonyl oxygen atom) the change in bonding is thought to be localized on the carbonyl subgroup and can be depicted by resonance form E. We note the caveat that using resonance structures for interpretation of excited states may be misleading and may not be a very accurate description. The use of the resonance structures here is only to facilitate a qualitative comparison of our present results to previous studies for other aromatic carbonyl compounds that used this framework for their interpretation. Within the A−D resonance form structures, the C and D forms characterize the ring-localized transition representing a typical $\pi\pi^*$ triplet, while the delocalized A and B forms depict a $\pi\pi^*$ triplet with somewhat biradical character. According to the evidence cited above, the triplet of HPA examined here and perhaps most acetophenone derivatives can be expressed properly by the delocalized forms A and B. It can be seen also from Figure 7 that the carbonyl CO bond retains some double bond character for a typical $\pi\pi^*$ triplet (C and D form) but become single-bond-like not only for a typical nπ^* triplet (form E) but also for the delocalized $\pi\pi^*$ triplet (forms A and B). Since the frequency of the CO stretching in the triplet is a direct reflection of the CO bond order, this implies that there will be no general correlation between the CO stretching frequency to the nature of the triplet. However, it is possible that the correlation suggested in some previous studies is applicable to aryl carbonyls that display typical nπ^* or $\pi\pi^*$ triplets that have CO stretching modes that are relatively pure and not strongly mixed with other modes.[55,57−60,74]

Conclusion

Picosecond and nanosecond time-resolved resonance Raman spectroscopy has been performed to study the structure and dynamics of the excited state of the phototrigger compound HPA in acetonitrile solvent. An oxygen-sensitive intermediate has been detected and was attributed to a $\pi\pi^*$ triplet of HPA with an estimated lifetime of ∼137 ns under nitrogen purge conditions. The triplet was found to be generated rapidly after photoexcitation, and we attributed the early picosecond spectral evolution to relaxation of the excess energy of the initially formed triplet produced from very rapid ISC conversion. These results tend to support the triplet mechanism for the HPA photodeprotection process reported in the literature. However, a very fast ESIPT process in the singlet state cannot be ruled out in aqueous environments and further experiments are needed to unambiguously determine whether one or both or some other mechanism is responsible for the deprotection process. DFT calculations were done for both the excited triplet and singlet ground states in order to elucidate the structures and vibrational frequencies. The calculated spectra reproduce the experimental ones reasonably well and were used to make tentative assignments to all the observed features. The observed frequency changes for the corresponding ground modes to those of the triplet correlate with the calculated structural changes between the two states. The major conformation change in the triplet compared with the ground state is at the *p*-hydroxyphenacyl

subgroup with the acetate moiety remaining almost unchanged. In the triplet, the ring-attached carbonyl CO bond lengthens significantly to have noticeable single-bond character; the ring shoulder CC bonds also become longer but the CC bond connecting the ring and the carbonyl shortens substantially. The triplet was found to be described properly by the $\pi\pi^*$ delocalized resonance forms for aromatic carbonyl compounds. The slightly twisted carbonyl conformation of the triplet was attributed to vibrational coupling with a nearby $n\pi^*$ triplet. This is consistent with the calculated vibrational frequency shifts associated with the ^{18}O and ^{13}C isotopic derivatives of the ring connected carbonyl. This is also consistent with the DFT calculation results in conjunction with experimental data that indicate there is no localized carbonyl CO stretching mode in the triplet and the identification of the experimental feature at 1260 cm^{-1} is a strongly mixed mode with contribution from the CO stretching.

Acknowledgment. We would like to thank the Research Grants Council of Hong Kong (Grants HKU 7108/02P and HKU 1/01C) to D.L.P. for support of this research. W.M.K. thanks the University of Hong Kong for the award of a Postdoctoral Fellowship.

References and Notes

(1) Bochet, C. G. *J. Chem. Soc., Perkin Trans. 1* **2002**, 125−142.
(2) Givens, R. S.; Kueper, L. W. *Chem. Rev.* **1993**, *93*, 55−66.
(3) Park, C. H.; Givens, R. S. *J. Am. Chem. Soc.* **1997**, *119*, 2453−2463, and references therein.
(4) Givens, R. S.; Athey, P. S.; Matuszewski, B.; Kueper, L. W., III; Xue, J. Y.; Fister, T. *J. Am. Chem. Soc.* **1993**, *115*, 6001−6012, and references therein.
(5) Givens, R. S.; Jung, A.; Park, C. H.; Weber, J.; Bartlett, W. *J. Am. Chem. Soc.* **1997**, *119*, 8369−8370.
(6) Givens, R. S.; Weber, J. F. W.; Conrad, P. G.; Orosz, G.; Donahue, S. L.; Thayer, S. A. *J. Am. Chem. Soc.* **2000**, *122*, 2687−2697, and references therein.
(7) Conrad, P. G.; Givens, R. S.; Weber, J. F. W.; Kandler, K. *Org. Lett.* **2000** *11*, 1545−1547.
(8) Conrad, P. G.; Givens, R. S.; Hellrung, B.; Rajesh, C. S.; Ramseier, M.; Wirz, J. *J. Am. Chem. Soc.* **2000**, *122*, 9346−9347.
(9) Givens, R. S.; Park, C. H. *Tetrahedron Lett.* **1996**, *37*, 6259−6262.
(10) Brousmiche, D. W.; Wan, P. *J. Photochem. Photobiol., A* **2000**, *130*, 133−118.
(11) Zhang, K.; Orrie, J. E. T.; Munasinghe, R. N.; Wan, P. *J. Am. Chem. Soc.* **1999**, *121*, 5625−5632.
(12) Banerjee, A.; Falvey, D. E. *J. Am. Chem. Soc.* **1998**, *120*, 2965−2966.
(13) Sheehan, J. C.; Umezawa, K. *J. Org. Chem.* **1973**, *38*, 3771.
(14) Epstein, W. W.; Garrossian, M. *J. Chem. Soc., Chem. Commun.* **1987**, 532.
(15) Baldwin, J. E.; McConnaughie, A. W.; Moloney, M. G.; Pratt, A. J.; Shim, S. B. *Tetrahedron* **1990**, *46*, 6879.
(16) Kwok, W. M.; Ma, C.; Matousek, P.; Parker, A. W.; Phillips, D.; Toner, W. T.; Towrie, M.; Umapathy, S. *J. Phys. Chem. A* **2001**, *105*, 984−990.
(17) Kwok, W. M.; Ma, C.; Parker, A. W.; Phillips, D.; Towrie, M.; Matousek, P.; Phillips, D. L. *J. Chem. Phys.* **2000**, *113*, 7471−7478.
(18) Kwok, W. M.; Ma, C.; Matousek, P.; Parker, A. W.; Phillips, D.; Toner, W. T.; Towrie, M.; Zuo, P.; Phillips, D. L. *Phys. Chem. Chem. Phys.* **2003**, *5*, 3643−3652.
(19) Ma, C.; Kwok, W. M.; Matousek, P.; Parker, A. W.; Phillips, D.; Toner, W. T.; Towrie, M. *J. Phys. Chem. A* **2001**, *105*, 4648−4652.
(20) Beck, S. M.; Brus, L. E. *J. Am. Chem. Soc.* **1982**, *104*, 1805−1808.
(21) Beck, S. M.; Brus, L. E. *J. Am. Chem. Soc.* **1982**, *104*, 4789−4792.
(22) Rossetti, R.; Brus, L. E. *J. Am. Chem. Soc.* **1986**, *108*, 4718−4720.
(23) Bisby, R. H.; Parker, A. W. *J. Am. Chem. Soc.* **1995**, *117*, 5664−5670.
(24) Rentzepis, P. M. *Science*, **1970**, *169*, 239−247.
(25) Ohmori, N.; Suzuki, T.; Ito, M. *J. Phys. Chem.* **1988**, *92*, 1086−1093.
(26) Wagner, P. J.; Kemppaninen, A. E.; Schott, H. N. *J. Am. Chem. Soc.* **1973**, *95*, 5604−5614.
(27) Dym. S.; Hochstrasser, R. M. *J. Chem. Phys.* **1969**, *51*, 2458−2468.
(28) Organero, J. A.; Tormo, L.; Douhal, A. *Chem. Phys. Lett.* **2002**, *363*, 409−414.
(29) Ameer-Beg, S.; Ormson, S. M.; Brown, R. G. *J. Phys. Chem. A* **2001**, *105*, 2709−3718.
(30) Folmer, D. E.; Wisniewski, E. S.; Stairs, J. R.; Casleman, A. W. *J. Phys. Chem. A* **2000**, *104*, 10545−10549.
(31) Arzhantsev, S. Y.; Takeuchi, S.; Tahara, T. *Chem. Phys. Lett.* **2000**, *330*, 83−90.
(32) Lu, C.; Hsieh, R. M. R.; Lee, I. R.; Cheng, P. Y. *Chem. Phys. Lett.* **1999**, *310*, 103−110.
(33) Mukaihata, H.; Nakagawa, T.; Kohtani, S.; Itoh, M. *J. Am. Chem. Soc.* **1994**, *116*, 10612−10618.
(34) Schwartz, B. J.; Peteanu, L. A.; Harris, C. B. *J. Phys. Chem.* **1992**, *96*, 3591−3598.
(35) Webb, S. P.; Phillips, L. A.; Yeh, S. W.; Tolbert, L. M.; Clark, J. H. *J. Phys. Chem.* **1986**, *90*, 5154−5164.
(36) Webb. S. P.; Yeh, S. W.; Phillips. L. A.; Tolbert, M. A.; Clark, J. H. *J. Am. Chem. Soc.* **1984**, *106*, 7286−7288.
(37) Wagner, P. J.; Hammond, G. S. *J. Am. Chem. Soc.* **1965**, *87*, 4009−4011.
(38) Baum. E. J.; Wan, J. K. S.; Pitts, J. N. *J. Am. Chem. Soc.* **1966**, *88*, 2652−2659.
(39) Yang, N. C.; McClure, D. S.; Murov, S. L.; Houser, J. J.; Dusenbery, R. *J. Am. Chem. Soc.* **1967**, *89*, 5466−5468.
(40) Rauh, R. D.; Leermakers, P. A. *J. Am. Chem. Soc.* **1968**, *90*, 2246−2249.
(41) Yang, N. C.; Dusenbery, R. L. *J. Am. Chem. Soc.* **1968**, *90*, 5899−5900.
(42) Wagner, P. J.; Kemppainen, A. E. *J. Am. Chem. Soc.* **1968**, *90*, 5898−5899.
(43) Yang, N. C.; Kimura, M.; Eisenhardt, W. *J. Am. Chem. Soc.* **1973**, *95*, 5058−5060.
(44) Wagner, P. J.; Truman, R. J.; Scaiano, J. C. *J. Am. Chem. Soc.* **1985**, *107*, 7, 7093−7097.
(45) Hirota, N. *Chem. Phys. Lett.* **1969**, *4*, 305−308.
(46) Cheng, T. H.; Hirota, N. *Chem. Phys. Lett.* **1972**, *13*, 194−198.
(47) Mao, S. W.; Wong, T. C.; Hirota, N. *Chem. Phys. Lett.* **1972**, *13*, 199−204.
(48) Lutz, H.; Bréhéretm, E.; Lindqvist, L. *J. Phys. Chem.* **1973**, *77*, 1758−1762.
(49) Lutz, H.; Duval, M. C.; Bréhéretm. E.; Lindzvist, L. *J. Phys. Chem.* **1972**, *76*, 821−822.
(50) Lim, E. C.; Li, Y. H.; Li, R. *J. Chem. Phys.* **1970**, *53*, 2443−2448.
(51) Li, Y. H.; Lim, E. C. *Chem. Phys. Lett.* **1970**, *7*, 15−18.
(52) Koyanagi, M.; Zwarich, R. J.; Goodman, L. *J. Chem. Phys.* **1972**, *56*, 3044−3060.
(53) Case, W. L.; Kearns, D. R. *J. Chem. Phys.* **1970**, *52*, 2175−2191.
(54) Kearns, D. R.; Case, W. A. *J. Am. Chem. Soc.* **1966**, *88*, 5087−5097.
(55) Tanaka, S.; Kato, C.; Horie, K.; Hamaguchi, H. *Chem. Phys. Lett.* **2003**, *381*, 385−391.
(56) Srivastava, S.; Yourd, E.; Toscano, J. P. *J. Am. Chem. Soc.* **1998**, *120*, 6173−6174.
(57) Sun, H.; Frei, H. *J. Phys. Chem. B* **1997**, *101*, 205−209.
(58) Tahara, T.; Hamaguchi, H.; Tasumi, M. *J. Phys. Chem.* **1990**, *94*, 170−178.
(59) Tahara, T.; Hamaguchi, H.; Tasumi, M. *J. Phys. Chem.* **1987**, *91*, 5875−5880.
(60) Tahara, T.; Hamaguchi, H.; Tasumi, M. *Chem. Phys. Lett.* **1988**, 135−139.
(61) Eijk, A. M. J. v.; Verhey, P. F. A.; Huizer, A. H.; Varma, C. A. G. O. *J. Am. Chem. Soc.* **1987**, *109*, 6635−6641.
(62) (a) Kwok, W. M.; Phillips, D. L. *J. Chem. Phys.* **1996**, *104*, 2529−2540. (b) Kwok, W. M.; Phillips, D. L. *J. Chem. Phys.* **1996**, *104*, 9816−9832. (c) Man, S. Q.; Kwok, W. M.; Johnson, A. E.; Phillips, D. L. *J. Chem. Phys.* **1996**, *105*, 5842−5857.
(63) (a) Kwok, W. M.; Phillips, D. L.; Yeung, P. K. Y.; Yam, V. W. W. *J. Phys. Chem. A* **1997**, *101*, 9286−9295. (b) Leung, K. H.; Phillips, D. L.; Tse, M. C.; Che, C. M.; Miskowski, V. M. *J. Am. Chem. Soc.* **1999**, *121*, 4799−4803. (c) Xia, B. H.; Zhang, H. X.; Che, C. M.; Leung, K. H.; Phillips, D. L.; Zhu, N.; Zhou, Z. Y. *J. Am. Chem. Soc.* **2003**, *125*, 10362−10374.
(64) (a) Li, Y.-L.; Leung, K. H.; Phillips, D. L. *J. Phys. Chem. A* **2001**, *105*, 10621−10625. (b) Li, Y.-L.; Chen, D.-M.; Phillips, D. L. *J. Org. Chem.* **2002**, *67*, 4228−4235. (c) Li, Y.-L.; Wang, D.; Phillips, D. L. *J. Chem. Phys.* **2002**, *117*, 7931−7941. (d) Ong, S. Y.; Chan, P. Y.; Zhu, P.; Leung, K. H.; Phillips, D. L. *J. Phys. Chem. A* **2003**, *107*, 3858−3865.
(65) Frisch, M. J.; Trucks, G. W.; Schlegel, H. B.; Scuseria, G. E.; Robb, M. A.; Cheeseman, J. R.; Zakrzewski, V. G.; Montgomery, J. A., Jr.; Stratmann, R. E.; Burant, J. C.; Dapprich, S.; Millam, J. M.; Daniels, A. D.; Kudin, K. N.; Strain, M. C.; Farkas, O.; Tomasi, J.; Barone, V.; Cossi,

M.; Cammi, R.; Mennucci, B.; Pomelli, C.; Adamo, C.; Clifford, S.; Ochterski, J.; Petersson, G. A.; Ayala, P. Y.; Cui, Q.; Morokuma, K.; Malick, D. K.; Rabuck, A. D.; Raghavachari, K.; Foresman, J. B.; Cioslowski, J.; Ortiz, J. V.; Baboul, A. G.; Stefanov, B. B.; Liu, G.; Liashenko, A.; Piskorz, P.; Komaromi, I.; Gomperts, R.; Martin, R. L.; Fox, D. J.; Keith, T.; Al-Laham, M. A.; Peng, C. Y.; Nanayakkara, A.; Gonzalez, C.; Challacombe, M.; Gill, P. M. W.; Johnson, B.; Chen, W.; Wong, M. W.; Andres, J. L.; Gonzalez, C.; Head-Gordon, M.; Replogle, E. S.; Pople, J. A. *Gaussian 98*, Revision A.7; Gaussian, Inc.: Pittsburgh, PA, 1998.

(66) Das, P. K.; Encinas, M. V.; Scaiano, J. C. *J. Am. Chem. Soc.* **1981**, *103*, 4154−4162.

(67) Unpublished work.

(68) Ma. C.; Kwok, W. M.; Matousek, P.; Parker, A. W.; Phillips, D.; Toner, W. T.; Towrie, M. *J. Raman Spectrosc.* **2001**, *32*, 115−123.

(69) Matousek, P.; Parker, A. W.; Towire, M.; Toner, W. T. *J. Chem. Phys*, **1997**, *107*, 9807−9817.

(70) Iwata, K.; Hamaguchi, H. J. *J. Phys. Chem. A* **1997**, *101*, 632−637.

(71) Hester, P. E.; Matousek, P.; Moore, J. N.; Parker, A. W.; Toner, W. T.; Towire, M. *Chem. Phys. Lett.* **1993**, *208*, 471−478.

(72) Weaver, W. L.; Huston, L. A.; Iwata, K. Gustafson, T. L. *J. Phys. Chem.* **1992**, *96*, 8956−8961.

(73) (a) Kwok, W. M.; Zhao, C.; Guan, X.; Li, Y.-L.; Du, Y.; Phillips, D. L. *J. Chem. Phys.* **2004**, *120*, 3323−3332. (b) Kwok, W. M.; Zhao, C.; Li, Y.-L.; Guan, X.; Wang, D.; Phillips, D. L. *J. Am. Chem. Soc.* **2004**, *126*, 3119−3131.

(74) George, M. W.; Kato, C.; Hamaguchi, H. *Chem. Lett.* **1993**, *5*, 873−876.

(75) Burgt, M. J. v. d.; Huizer, A. H.; Varma, C. A. G. O.; Wanger, B. D.; Lusztyk, J. *Chem. Phys.* **1995**, *196*, 193−210.

(76) Porter, G.; Suppan, P. *Trans. Faraday Soc.* **1965**, *61*, 1664−1673.

(77) Beckett, A.; Porter, G. *Trans. Faraday Soc.* **1963**, *59*, 2051−2057.